

## Sensitive dependence of isotope and isobar distributions of limiting temperatures on the symmetry energy

Li Ou,<sup>1,\*</sup> Min Liu,<sup>1</sup> and Zhuxia Li<sup>2</sup>

<sup>1</sup>College of Physics and Technology, Guangxi Normal University, Guilin 541004, People's Republic of China

<sup>2</sup>China Institute of Atomic Energy, Beijing 102413, People's Republic of China

(Received 13 October 2013; revised manuscript received 20 November 2013; published 27 January 2014)

The mass, isotope, and isobar distributions of limiting temperatures for finite nuclei are investigated by using a thermodynamics approach together with the Skyrme energy density functional. The relationship between the width of the isotope (isobar) distribution of limiting temperatures and the stiffness of the density dependence of the symmetry energy clearly is observed. The nuclear symmetry energy with smaller slope parameter  $L_{\text{sym}}$  causes a wider isotope (isobar) distribution of limiting temperatures. The widths of the isotope (isobar) distributions of limiting temperatures could be useful observables for exploring the information of the density dependence of the nuclear symmetry energy at finite temperatures.

DOI: 10.1103/PhysRevC.89.011001

PACS number(s): 21.30.Fe, 21.65.Ef, 24.10.-i

The nuclear symmetry energy plays a crucial role for understanding nuclear phenomena and for exploring the equation of state (EOS) for isospin asymmetric nuclear matter. Significant efforts have been devoted to constrain the symmetry energy at both high densities [1,2] and subsaturation densities [3–8]. Up to now, some constraints on symmetry energy at subnormal densities have already been obtained from different experimental measurements that include nuclear structure and reactions [6,9–13]. However, the uncertainties of the density dependence of nuclear symmetry energy are still large. More information on the nuclear symmetry energy is still required for understanding the structures of nuclei far away from the  $\beta$ -stability line, heavy-ion collisions, supernova explosions, and neutron star properties [14,15].

The energy per nucleon in uniform nuclear matter can be written as  $E(\rho, \delta) = E_0(\rho, \delta = 0) + E_{\text{sym}}(\rho)\delta^2$ , where  $\delta = (\rho_n - \rho_p)/\rho$  and  $\rho_n$ ,  $\rho_p$ , and  $\rho$  are the neutron, proton, and nucleon densities, respectively.  $E_{\text{sym}}(\rho)$  describes the density dependence of the symmetry energy and can be expanded as

$$E_{\text{sym}}(\rho) = E(\rho_0) + \frac{L_{\text{sym}}}{3} \left( \frac{\rho - \rho_0}{\rho_0} \right) + \frac{K_{\text{sym}}}{18} \left( \frac{\rho - \rho_0}{\rho_0} \right)^2 + \dots, \quad (1)$$

where  $L_{\text{sym}} = 3\rho_0 \frac{\partial E_{\text{sym}}(\rho)}{\partial \rho} |_{\rho_0}$  and  $K_{\text{sym}} = 9\rho_0^2 \frac{\partial^2 E_{\text{sym}}(\rho)}{\partial \rho^2} |_{\rho_0}$  denote the slope and curvature parameters, respectively. On the other hand, the symmetry energy also depends on the temperature, which is also of fundamental importance for the liquid-gas phase transition of asymmetric nuclear matter, the dynamical evolution mechanisms of massive stars, and the supernova explosion. The behavior of the temperature dependence of the symmetry energy is less well understood [16–20], which compares the symmetry energy at zero temperature.

It is found that the calculated limiting temperature sensitively depends on the stiffness of the EOS (the incompressibility), critical temperature, surface tension, *et al.* [21–24]. From experimental observations of limiting temperature, Natowitz *et al.* successfully derived the critical temperature and the incompressibility of isospin symmetric nuclear matter [25,26]. Furthermore, Li and Liu [24] pointed out that the isotope distribution of limiting temperatures sensitively depended on the isospin-dependent part of the interaction. But the effects of the isoscalar and isovector parts of the EOS on limiting temperature are entangled in their paper. In this Rapid Communication, to manifest the isospin effect, we first investigate the limiting temperatures of nuclei in isotope and isobar chains. Then we investigate the correlation between the isotope (isobar) distribution of the limiting temperatures and the density dependence of symmetry energy. In addition, we attempt to extract the information of the density dependence of symmetry energy at finite temperatures from available experimental data.

We use the same model as that used in Refs. [24,27,28]. Within this model, a hot nucleus is considered as a spherical liquid droplet of uniformly distributed nuclear matter at constant temperature. This liquid droplet is in thermal equilibrium with the surrounding vapor. The thermal, mechanical, and chemical equilibria between the liquid droplet and the surrounding vapor are required, which leads to a set of standard coexistence equations,

$$\mu_p(T, \rho_L, \delta_L) = \mu_p(T, \rho_V, \delta_V), \quad (2)$$

$$\mu_n(T, \rho_L, \delta_L) = \mu_n(T, \rho_V, \delta_V), \quad (3)$$

$$P(T, \rho_L, \delta_L) = P(T, \rho_V, \delta_V). \quad (4)$$

The subscript  $L$  refers to the liquid droplet, and the subscript  $V$  refers to the surrounding vapor. For simplification, the Coulomb interaction is screened in the calculation of the pressure and the proton chemical potential of the surrounding vapor. The maximum temperature at which the coexistence equations have solutions is the limiting temperature. The chemical potential of the nucleon of species  $q$  can be

\*only.ouli@gmail.com

written as

$$\mu_q(T, \rho, \delta) = u_q(T, \rho, \delta) + T \sum_{n=1}^{\infty} \frac{n+1}{n} b_n (1 \pm \delta)^n \left( \frac{\lambda_T^3}{g_{s,l}} \rho \right)^n + T \ln(1 \pm \delta) + T \ln \frac{\lambda_T^3}{g_{s,l}} \rho + \varepsilon_{\text{Coul}} \delta_{q,p}, \quad (5)$$

where the “+” symbol stands for neutrons and the “−” symbol stands for protons. The  $\lambda_T$  is the effective thermal wavelength of the nucleon, which reads

$$\lambda_T = \left( \frac{2\pi \hbar^2}{m_q^* T} \right)^{1/2}. \quad (6)$$

$m_q^*$  and  $u_q$  are the effective mass and the single-particle potential energy, respectively,  $b_n$ 's are the coefficients of the virial series for the ideal Fermi gas,  $g_{s,l} = 4$  is the spin-isospin degeneracy, and  $\varepsilon_{\text{Coul}}$  is the Coulomb energy term. The total pressure of the droplet is written as

$$P(T, \rho, \delta) = P_{\text{bulk}} + P_{\text{Coul}} + P_{\text{surf}}. \quad (7)$$

The bulk pressure of the nucleus can be calculated by [29]

$$P_{\text{bulk}} = \sum_q \left[ \left( \frac{5}{3} \frac{1}{2m_q^*} - \frac{1}{2m_q} \right) \hbar^2 \tau_q + \frac{1}{2} u_q \rho (1 \pm \delta) \right] - U, \quad (8)$$

where  $U$  and  $\tau_q$  in  $P_{\text{bulk}}$  are the potential density and the kinetic-energy density of the nucleon, respectively,  $P_{\text{Coul}}$  is the pressure contributed by the Coulomb interaction, and  $P_{\text{surf}}$  is the pressure contributed by the surface tension that includes a symmetry-surface term suggested in Refs. [30,31,36] (which is called Surf2 in Ref. [24]). The critical temperature for infinite nuclear matter is taken as 17 MeV, referenced from Ref. [26] where  $T_c = 16.6 \pm 0.86$  MeV.

The effective Skyrme interaction is adopted in this Rapid Communication, and the expressions of  $m_q^*$ ,  $u_q$ , and  $\tau_q$  can be found in Ref. [24]. To study the effect of symmetry energy on limiting temperature, 29 sets of Skyrme interactions are selected in the calculations with the values of incompressibility  $K_{\infty} = 230 \pm 30$  MeV and quite different values of  $L_{\text{sym}}$  and  $K_{\text{sym}}$ . In Table I, we list the slope parameter  $L_{\text{sym}}$ , asymmetry coefficient  $a_s$  at temperatures of  $T = 0/5$  MeV, curvature parameter  $K_{\text{sym}}$ , and incompressibility module  $K_{\infty}$  at temperature of  $T = 0$  MeV, predicted by these Skyrme interactions. The Skyrme interactions are sorted by the ascending order with slope parameter  $L_{\text{sym}}$  at zero temperature.

Figure 1 presents the density dependence of the symmetry energy with some Skyrme interactions, which describe the possible behavior of the symmetry energy predicted by different theories. Especially, we select the Skz-series because these interactions have almost the same isoscalar part but varied isovector part in the EOS, which are especially useful for studying the symmetry energy effect.

Figure 2 shows the mass distributions of limiting temperatures of nuclei along the  $\beta$ -stability line with  $Z = 0.5A - 3 \times 10^{-3} A^{5/3}$ , calculated with different Skyrme interactions. The data, which are extracted from a number of different

TABLE I. Slope parameter  $L_{\text{sym}}$ , asymmetry coefficient  $a_s$  at temperatures of  $T = 0/5$  MeV, curvature parameter  $K_{\text{sym}}$ , and incompressibility module  $K_{\infty}$  at temperature of  $T = 0$  MeV, predicted by different Skyrme interactions.

Version	$L_{\text{sym}}$	$a_s$	$K_{\text{sym}}$	$K_{\infty}$
SkM1 [32]	−31.17/−29.95	26.48/26.22	−383	216
SVII [33]	−9.28/−7.89	27.86/27.46	−488	367
Skz4 [34]	4.89/6.17	32.36/31.78	−246	230
Skz3 [34]	14.19/15.37	32.80/32.31	−243	230
Skz2 [34]	20.50/21.59	33.31/32.96	−256	230
Skz1 [34]	33.06/34.17	33.66/33.46	−235	230
BSk9 [35]	40.24/41.37	30.79/30.22	−148	231
Skz0 [34]	42.56/44.02	34.09/34.14	−231	230
SLy7 [36]	47.72/48.92	32.91/32.41	−116	230
SkM* [37]	50.13/51.34	31.46/31.20	−151	216
SkT3 [38]	56.77/57.73	32.20/31.62	−134	236
SkT2 [38]	57.58/58.54	32.70/32.12	−136	236
SkT1 [38]	57.60/58.56	32.72/32.14	−136	236
KDE0v1 [39]	58.92/60.11	35.55/35.04	−130	232
SKRA [40]	59.96/58.09	32.72/32.45	−133	214
SQMC650 [41]	59.65/60.89	35.04/34.82	−168	222
SV-sym32 [42]	61.09/62.61	33.62/33.41	−144	233
Skz-1 [34]	62.40/64.16	34.27/34.44	−171	230
NRAPR [15]	62.45/63.53	33.40/33.11	−117	222
LNS [43]	62.65/63.75	34.41/34.07	−127	214
SQMC700 [41]	63.67/64.81	34.20/33.92	−133	214
MSL0 [44]	64.21/65.36	31.55/31.21	−97	233
Ska35s20 [45]	65.06/66.00	34.59/34.01	−122	240
Ska25s20 [45]	66.58/67.56	34.93/34.35	−120	221
Skxs20 [46]	72.55/73.59	37.27/36.74	−123	207
SkO [47]	81.70/82.79	32.95/32.47	−43	224
SkT5 [38]	100.11/101.09	37.10/36.52	−26	202
SkI5 [48]	128.01/128.70	36.11/35.60	156	256
SkI1 [48]	160.74/161.91	38.24/37.73	234	244

experimental measurements and only for symmetric or slightly asymmetric nuclei, are taken from Refs. [25,26].

From Fig. 2, one can see the influence of  $K_{\infty}$  on the limiting temperature. The calculation with the stiffer EOS

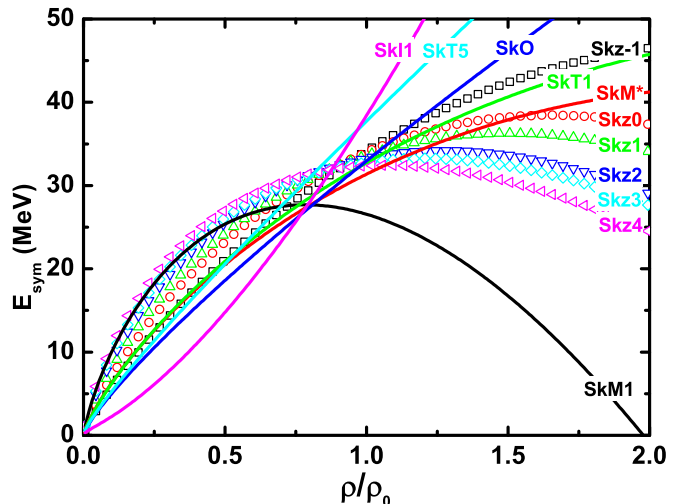


FIG. 1. (Color online) Density dependence of symmetry energy with various Skyrme interactions.

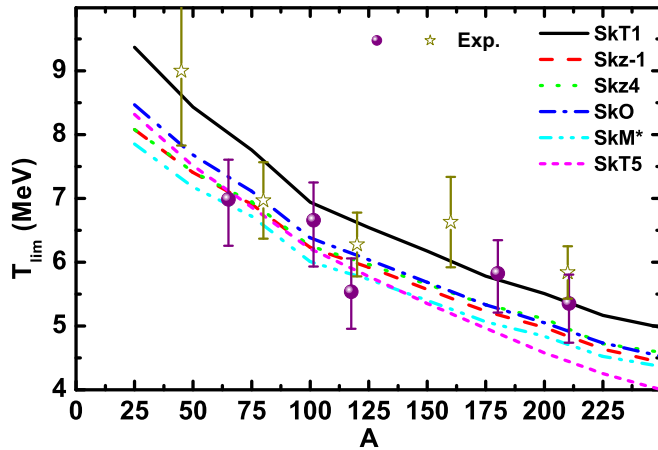


FIG. 2. (Color online) Mass distributions of the limiting temperatures for  $\beta$ -stability nuclei calculated with different Skyrme interactions.

obtains the higher limiting temperature, which is consistent with other investigations [22–24]. As expected, the behavior of the symmetry energy does not significantly influence the mass dependence of the limiting temperatures for the  $\beta$ -stability nuclei. For example, the calculation results with Skz-1 and Skz4 are almost the same, although the corresponding isovector parts are quite different. To reveal the isospin energy effect more clearly, we further study the limiting temperatures of nuclei in isotope and isobar chains.

Figure 3 shows the isotope distributions of limiting temperatures for Sn isotopes calculated with Skz-series Skyrme interactions. From the figure, one can see that all isotope distributions of limiting temperatures appear to be inverted parabolas. On the left side of the parabolas, the limiting temperatures of the nuclei increase with the neutron numbers since the Coulomb potential is reduced. On the right side, the limiting temperature decreases with the extra richness of the neutrons because the nuclei become unstable due to

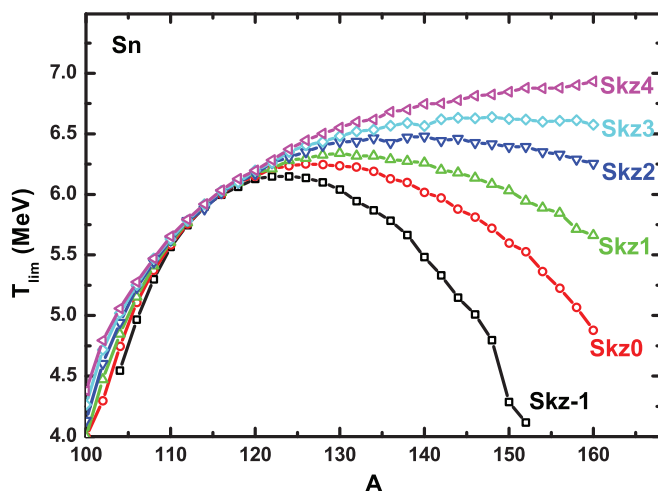


FIG. 3. (Color online) Isotope distributions of the limiting temperatures for Sn calculated with Skz-series Skyrme interactions.

symmetry energy that is too strong. The competition between the Coulomb energy and the symmetry energy leads to the parabolic shape of the isotope distribution. All the curves intercross around  $^{116}\text{Sn}$ , which is the corresponding  $\beta$ -stability isotope of Sn. This is due to the fact that the parameters of each Skz interaction are fitted to the properties of nuclei near the  $\beta$ -stability line. Furthermore, all Skz interactions have the same isoscalar part in the EOS, which leads to the similar behaviors for the  $\beta$ -stability nuclei. For the isotopes far away from the  $\beta$ -stability line, the difference between the limiting temperatures calculated with different Skz interactions becomes large. The most clear and interesting feature shown in Fig. 3 is as follows: The softer the symmetry energy is, the broader the distribution of the limiting temperature is, and we get a higher limiting temperature for the neutron-rich isotope.

To understand the effect of symmetry energy on the limiting temperature, in Fig. 4, we present the correlations of  $\mu_n \sim P$  and  $\mu_p \sim P$  for  $^{136}\text{Sn}$  and the surrounding vapor at  $T = 5, 6.5,$  and  $8$  MeV calculated with Skz4 and Skz-1, respectively. Since the isospin asymmetry  $\delta_V$  is not fixed, we take three different values  $\delta_V = 0.0, 0.5,$  and  $0.8$ . One can find that the proton and neutron chemical potentials for the vapor (which

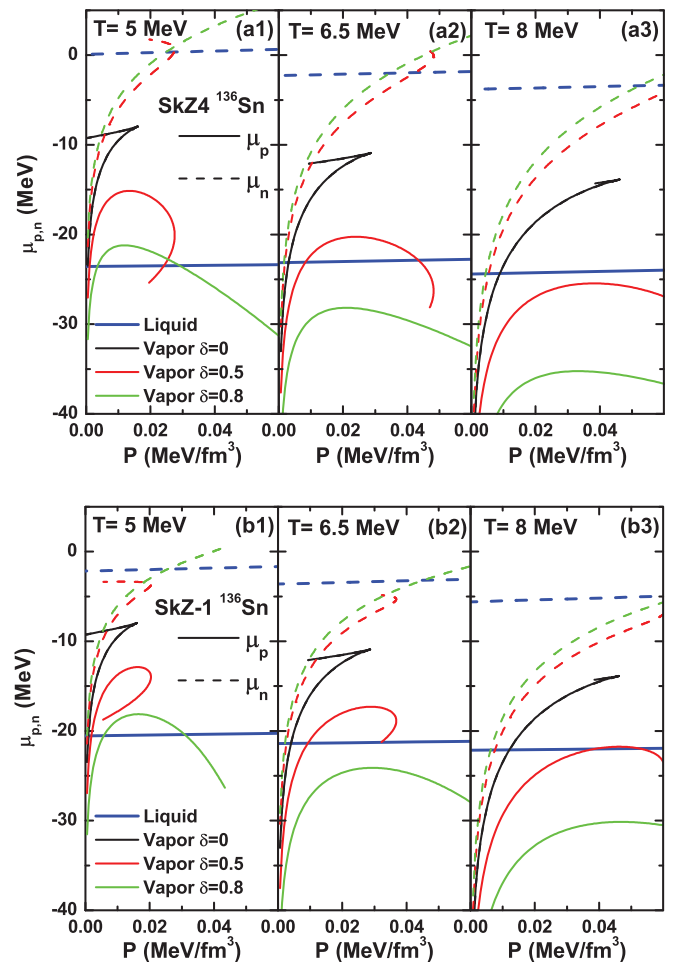


FIG. 4. (Color online) Correlations of  $\mu_n \sim P$  and  $\mu_p \sim P$  for the  $^{136}\text{Sn}$  nucleus and surrounding vapor at  $T = 5, 6.5,$  and  $8$  MeV, calculated with Skz4 (upper panel) and Skz-1 (bottom panel).

is low density and neutron rich) decrease with temperature. The neutron chemical potential of the vapor is higher, and the proton chemical potential of the vapor is lower with Skz4 than the corresponding results by using Skz1 because the symmetry energy for Skz4 is much softer than that for Skz-1. If the solution for coexistence equations exists, there simultaneously should be intersects between the liquid and the vapor curves for both  $\mu_n \sim P$  and  $\mu_p \sim P$ . Because of the effect of the symmetry energy, one sees that, in Figs. 4(a1) and 4(b1) at  $T = 5$  MeV, there simultaneously exist intersects for  $\mu_n \sim P$  and  $\mu_p \sim P$  with  $\delta_V = 0.5$  and  $0.8$  for the Skz4 case but only at  $\delta_V = 0.8$  for the Skz-1 case. In Figs. 4(a2) and 4(b2) at  $T = 6.5$  MeV, there simultaneously exist intersects for  $\mu_n \sim P$  and  $\mu_p \sim P$  at  $\delta_V = 0.5$ , and intersects do not exist for  $\delta_V = 0.8$  with Skz4 because the proton chemical potential with  $\delta_V = 0.8$  is reduced too much. For the Skz-1 case, there simultaneously is no intersect for the  $\mu_n \sim P$  and  $\mu_p \sim P$  curves. At  $T = 8$  MeV, there simultaneously is no intersect between the liquid and the vapor curves for  $\mu_n \sim P$  and  $\mu_p \sim P$  because the vapor  $\mu_p \sim P$  curve becomes too low to cross over the liquid  $\mu_p \sim P$  curve for the Skz4 case and, for the Skz-1 case, the vapor  $\mu_n \sim P$  curve becomes too low to cross over the liquid  $\mu_n \sim P$  curve. From the above discussions, it can be understood that the softer symmetry energy increases the  $\mu_n$  of the vapor, which makes it possible for the vapor to be in equilibrium with the liquid at a higher temperature. Thus, the higher limiting temperature is obtained for the softer symmetry energy case.

The experiment S254, conducted at the SIS heavy-ion synchrotron at GSI Darmstadt, was devoted to study the isotope effects in projectile fragmentation at relativistic energy [49]. The collisions of 600 MeV/nucleon  $^{124}\text{Sn}$ ,  $^{107}\text{Sn}$ , and  $^{124}\text{La}$  on  $^{\text{nat}}\text{Sn}$  were performed, the limiting temperatures for nuclei with the same  $A/Z$  but  $Z_{\text{bound}}/Z_{\text{proj}}$  intervals [0.6,0.8] for  $^{124}\text{Sn}$  and [0.55,0.75] for the neutron-poor cases ( $^{107}\text{Sn}$  and  $^{124}\text{La}$ ) were extracted. According to this experimental measurement, the spectator systems are most likely populated in the bin of nuclei with the same  $A/Z$  but only 75% of the projectile mass [49,50]. Thus, we investigate the limiting temperatures for the isotope chain of  $_{38}\text{Sr}$  and the isobar chain of  $^{93}\text{A}$  by attempting to obtain some information on the density dependence of the symmetry energy at finite temperatures with these data.

Figure 5 presents the isotope distributions of limiting temperatures for Sr calculated with various Skyrme interactions. The data are taken from Ref. [49]. One can see that all Skz family interactions fail to reproduce the experimental data for  $^{80,93}\text{Sr}$ . The results are overestimated. It seems that the symmetry energy is too soft. To describe the experimental data, more interactions with various stiffnesses of symmetry energy, which include those suggested by Dutra *et al.* [45], are included in the calculations. It seems that the results with SkT5 reproduce the data reasonably well. However, the calculation results look a little messy, even if just the partial results are shown in the figure. We believe that this chaos is caused mainly by different isoscalar parts of the EOS as shown in Fig. 2. It is known that both the isovector and the isoscalar parts influence the results. To reduce the influence from the isoscalar part of the interaction, we only concentrate on the shapes of the isotope distributions of limiting temperatures rather than their

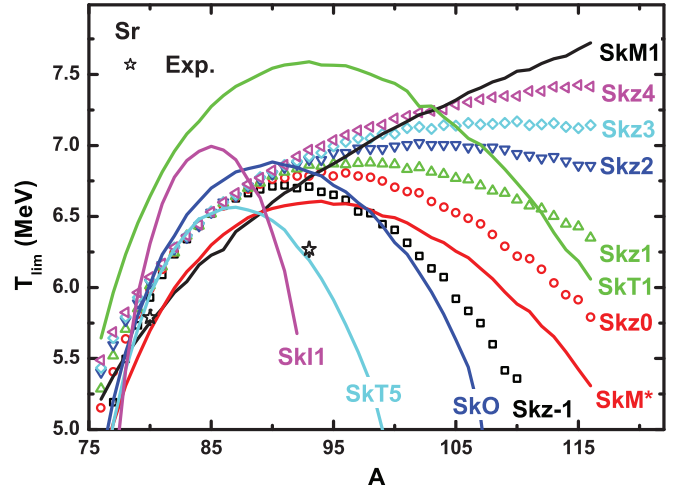


FIG. 5. (Color online) Isotope distributions of the limiting temperatures for Sr calculated with various Skyrme interactions.

absolute values. To quantitatively describe the shape of the distribution, we introduce the width of distribution  $\sigma$ .  $\sigma$  is obtained by fitting the isotope distribution of limiting temperatures with a three-parameter Gaussian function,

$$g(A) = \frac{a}{\sqrt{2\pi}\sigma} \exp\left[-\frac{(A - A_c)^2}{2\sigma^2}\right]. \quad (9)$$

The correlation between distribution width  $\sigma$  and  $L_{\text{sym}}$  of the symmetry energy is illustrated in the inner figure in Fig. 6. One can see that a softer symmetry energy obtains a wider distribution of the limiting temperature, which is independent on the isoscalar part of the EOS. We also note that there are some fluctuations for width  $\sigma$  within the range of  $L_{\text{sym}}$  from 48 to 65 MeV. To explore the reason for the fluctuation, we show the results in the enlarged image. For each calculated point, we present the label of the Skyrme interaction, the effective mass ( $m^*/m$ ), and the effective mass splitting (EMS) ratio

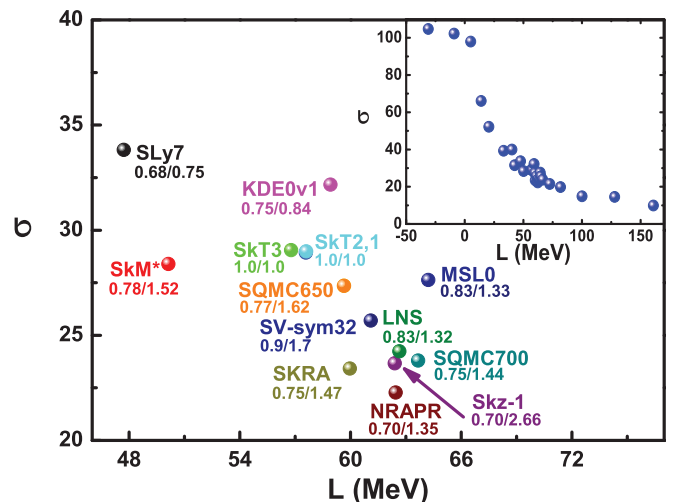


FIG. 6. (Color online) Correlation between distribution width  $\sigma$  and  $L_{\text{sym}}$  of the symmetry energy, see the text for details.



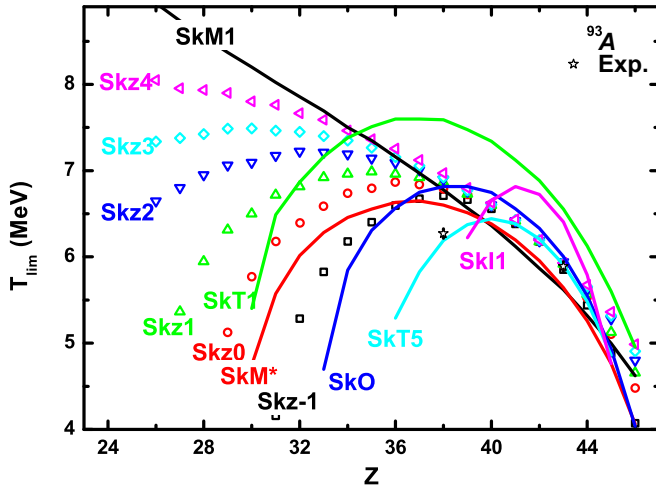


FIG. 7. (Color online) Isobar distributions of the limiting temperatures for  $^{93}A$  calculated with various Skyrme interactions.

( $m_n^*/m_p^*$ ) at the saturation density. It seems that the fluctuations have a certain relation with the EMS. From the figure, we find that, for the Skyrme interactions with similar  $L_{\text{sym}}$  values, the Skyrme interactions with  $m_n^* < m_p^*$  (SLy7, KDE0v1) obtain larger  $\sigma$ 's, and those with  $m_n^* > m_p^*$  obtain smaller  $\sigma$ 's. It is actually understandable as the kinetic energy also contributes to the chemical potential and pressure of the nuclei in which the effective mass of the proton (neutron) is involved.

We perform the same calculations for the isobar chain of  $^{93}A$ . From the results for the  $^{93}A$  isobar shown in Fig. 7, the consistent conclusion can be obtained as that for the Sn isotopes, i.e., the softer symmetry energy obtains a wider distribution of limiting temperature.

These investigations indicate that the widths of the isotope and isobar distributions of limiting temperatures are closely correlated to the density dependence of the symmetry energy at finite temperatures. The neutron-proton EMS also has certain influences on the widths of the isotope and isobar distributions of limiting temperatures, which can also provide us with information for the neutron-proton EMS. From Figs. 5 and 7, we note that the curves calculated with SkT5 roughly pass through the data points for  $^{80}\text{Sr}$ ,  $^{93}\text{Sr}$ , and  $^{93}\text{Tc}$  and a better agreement is obtained compared with other interactions. As

$L_{\text{sym}}$  and  $a_s$  are correlated, some investigations produce a range of acceptable values (see Ref. [9] for a recent summary). The values of  $L_{\text{sym}}$  and  $a_s$  for SkT5 are located at the large side of the acceptable values. Moreover, see Fig. 1, the SkT5 has the symmetry energy almost linearly depending on density (i.e., the small  $K_{\text{sym}}$ , which is even less constrained up to now). However, as we know that the limiting temperature depends on both the isoscalar and the isovector parts, the symmetry energy cannot be constrained uniquely by two data points in the isotope and isobar distributions of the limiting temperatures. To obtain the experimental information for the width of the isotope (isobar) distribution of limiting temperatures, at least three points are needed. Thus, at least one more datum is required to determine the width of distribution in addition to  $^{80,93}\text{Sr}$  or  $^{93}\text{Sr}$  and  $^{93}\text{Tc}$ . For this purpose,  $^{83}\text{Sr}$ – $^{86}\text{Sr}$  or  $^{93}_{40}\text{A}$ – $^{93}_{42}\text{A}$  should be the best candidates.

To summarize, the mass, isotope, and isobar distributions of limiting temperatures are investigated by using 29 sets of Skyrme interactions. The correlation between the width of the isotope (isobar) distribution of limiting temperatures and the slope parameter  $L_{\text{sym}}$  of the symmetry energy clearly is observed from the calculations. A softer symmetry energy causes a wider isotope (isobar) distribution of limiting temperatures. The neutron-proton EMS also slightly influences the width of the distribution. As a helpful observable, the width of the isotope (isobar) distribution of limiting temperatures should be measured for obtaining the information of the isovector part of the EOS, not only the momentum-independent part, but also the momentum-dependent part. With concern for the available experimental data of the isotope Sr and isobar  $^{93}A$  chains, at least one more datum point is required to determine the width of the distribution. For this purpose,  $^{83}\text{Sr}$ – $^{86}\text{Sr}$  or  $^{93}_{40}\text{A}$ – $^{93}_{42}\text{A}$  should be the best candidates in addition to  $^{80,93}\text{Sr}$  or  $^{93}\text{Sr}$  and  $^{93}\text{Tc}$ .

We thank Professor N. Wang for a careful reading of the manuscript. This work was supported by the National Natural Science Foundation of China (under Grants No. 11005022, No. 11365004, No. 11365005, No. 11075215, No. 11005003, No. 11275052, and No. 11375062), was supported partly by MOST of China (973 Program with Grant No. 2013CB834404) and by the Doctor Startup Foundation of Guangxi Normal University.

- [1] P. Danielewicz, R. Lacey, and W. G. Lynch, *Science* **298**, 1592 (2002).
- [2] C. Fuchs, *Prog. Part. Nucl. Phys.* **56**, 1 (2006).
- [3] M. B. Tsang *et al.*, *Phys. Rev. Lett.* **92**, 062701 (2004).
- [4] T. X. Liu *et al.*, *Phys. Rev. C* **76**, 034603 (2007).
- [5] M. A. Famiano *et al.*, *Phys. Rev. Lett.* **97**, 052701 (2006).
- [6] M. B. Tsang, Y. Zhang, P. Danielewicz, M. Famiano, Z. Li, W. G. Lynch, and A. W. Steiner, *Phys. Rev. Lett.* **102**, 122701 (2009).
- [7] P. Danielewicz and J. Lee, *Nucl. Phys. A* **818**, 36 (2009).
- [8] P. M. Walker, S. Lalkovski, and P. D. Stevenson, *Phys. Rev. C* **81**, 041304 (2010).
- [9] M. B. Tsang, J. R. Stone, F. Camera *et al.*, *Phys. Rev. C* **86**, 015803 (2012).
- [10] A. Klimkiewicz, N. Paar, P. Adrich *et al.*, *Phys. Rev. C* **76**, 051603 (2007).
- [11] M. Centelles, X. Roca-Maza, X. Viñas, and M. Warda, *Phys. Rev. Lett.* **102**, 122502 (2009).
- [12] M. Baldo, C. Maieron, P. Schuck, and X. Viñas, *Nucl. Phys. A* **736**, 241 (2004).
- [13] M. Liu, N. Wang, Z.-X. Li, and F.-S. Zhang, *Phys. Rev. C* **82**, 064306 (2010).
- [14] B.-A. Li, L.-W. Chen, and C. M. Ko, *Phys. Rep.* **464**, 113 (2008).
- [15] A. W. Steiner, M. Prakash, J. M. Lattimer, and P. J. Ellis, *Phys. Rep.* **411**, 325 (2005).
- [16] J. Xu, L.-W. Chen, B.-A. Li, and H.-R. Ma, *Phys. Rev. C* **75**, 014607 (2007); **77**, 014302 (2008).

- [17] B.-A. Li and L.-W. Chen, *Phys. Rev. C* **74**, 034610 (2006).
- [18] S. Kowalski, J. B. Natowitz, S. Shlomo *et al.*, *Phys. Rev. C* **75**, 014601 (2007).
- [19] C. C. Moustakidis, *Phys. Rev. C* **76**, 025805 (2007).
- [20] L. Ou, Z. Li, Y. Zhang, and M. Liu, *Phys. Lett. B* **697**, 246 (2011).
- [21] J. B. Natowitz, K. Hagel, R. Wada, Z. Majka, P. Gonthier, J. Li, N. Mdeiwayeh, B. Xiao, and Y. Zhao, *Phys. Rev. C* **52**, R2322 (1995).
- [22] H. Q. Song and R. K. Su, *Phys. Rev. C* **44**, 2505 (1991).
- [23] A. Kelic, J. B. Natowitz, and K.-H. Schmidt, *Eur. Phys. J. A* **30**, 203 (2006).
- [24] Z. Li and M. Liu, *Phys. Rev. C* **69**, 034615 (2004).
- [25] J. B. Natowitz, R. Wada, K. Hagel, T. Keutgen, M. Murray, A. Makeev, L. Qin, P. Smith, and C. Hamilton, *Phys. Rev. C* **65**, 034618 (2002).
- [26] J. B. Natowitz, K. Hagel, Y. Ma, M. Murray, L. Qin, R. Wada, and J. Wang, *Phys. Rev. Lett.* **89**, 212701 (2002).
- [27] M. Liu, Z.-X. Li, and J.-F. Liu, *Chin. Phys. Lett.* **20**, 1706 (2003).
- [28] H. R. Jaqaman, *Phys. Rev. C* **39**, 169 (1989); **40**, 1677 (1989).
- [29] S. J. Lee and A. Z. Mekjian, *Phys. Rev. C* **63**, 044605 (2001).
- [30] E. Chabanat, P. Bonche, P. Haensel, J. Meyer, and R. Schaeffer, *Nucl. Phys. A* **627**, 710 (1997).
- [31] W. D. Myers, and W. J. Świątecki, *Nucl. Phys.* **81**, 1 (1966).
- [32] J. M. G. Gómez and M. Casas, *Few-Body Syst., Suppl.* **8**, 374 (1995); X. Li and P.-H. Heenen, *Phys. Rev. C* **54**, 1617 (1996).
- [33] M. J. Giannoni and P. Quentin, *Phys. Rev. C* **21**, 2076 (1980).
- [34] J. Margueron, J. Navarro, and N. V. Giai, *Phys. Rev. C* **66**, 014303 (2002).
- [35] S. Goriely, M. Samyn, J. M. Pearson, and M. Onsi, *Nucl. Phys. A* **750**, 425 (2005).
- [36] E. Chabanat, P. Bonche, P. Haensel, J. Meyer, and R. Schaeffer, *Nucl. Phys. A* **635**, 231 (1998).
- [37] J. Bartel, P. Quentin, M. Brack, C. Guet, and H.-B. Hakansson, *Nucl. Phys. A* **386**, 79 (1982).
- [38] F. Tondeur, M. Brack, M. Farine, and J. M. Pearson, *Nucl. Phys. A* **420**, 297 (1984).
- [39] B. K. Agrawal, S. Shlomo, and V. K. Au, *Phys. Rev. C* **72**, 014310 (2005).
- [40] J. M. G. Gómez, C. Prieto, and J. Navarro, *Nucl. Phys. A* **549**, 125 (1992).
- [41] P. A. M. Guichon, H. H. Matevosyan, N. Sandulescu, and A. W. Thomas, *Nucl. Phys. A* **772**, 1 (2006).
- [42] P. Klüpfel, P.-G. Reinhard, T. J. Bürvenich, and J. A. Maruhn, *Phys. Rev. C* **79**, 034310 (2009).
- [43] L. G. Cao, U. Lombardo, C. W. Shen, and N. V. Giai, *Phys. Rev. C* **73**, 014313 (2006).
- [44] L.-W. Chen, C. M. Ko, B.-A. Li, and J. Xu, *Phys. Rev. C* **82**, 024321 (2010).
- [45] M. Dutra, O. Lourenço, J. S. Sá Martins, A. Delfino, J. R. Stone, and P. D. Stevenson, *Phys. Rev. C* **85**, 035201 (2012).
- [46] B. A. Brown, G. Shen, G. C. Hillhouse, J. Meng, and A. Trzcińska, *Phys. Rev. C* **76**, 034305 (2007).
- [47] P.-G. Reinhard *et al.*, *Phys. Rev. C* **60**, 014316 (1999).
- [48] P.-G. Reinhard and H. Flocard, *Nucl. Phys. A* **584**, 467 (1995).
- [49] C. Sfienti *et al.* (ALADIN2000 Collaboration), *Phys. Rev. Lett.* **102**, 152701 (2009).
- [50] J. Pochodzalla *et al.*, *Phys. Rev. Lett.* **75**, 1040 (1995).